═══REVIEW COMMONS MANUSCRIPT═══

IMPORTANT:

- Manuscripts submitted to Review Commons are peer reviewed in a journal-agnostic way.
- Upon transfer of the peer reviewed preprint to a journal, the referee reports will be available in full to the handling editor.
- The identity of the referees will NOT be communicated to the authors unless the reviewers choose to sign their report.
- The identity of the referee will be confidentially disclosed to any affiliate journals to which the manuscript is transferred.

GUIDELINES:

- For reviewers: https://www.reviewcommons.org/reviewers
- For authors: https://www.reviewcommons.org/authors

CONTACT:

The Review Commons office can be contacted directly at: office@reviewcommons.org

Virtual Colon: Spatiotemporal modelling of metabolic interactions in a computational colonic environment

Georgios Marinos[1,*], Johannes Zimmermann[1,2,3*], Jan Taubenheim[1], and Christoph Kaleta[1,$]

[1] Research Group Medical Systems Biology, University Hospital Schleswig-Holstein Campus Kiel, Kiel University, Kiel, Schleswig-Holstein, Germany

[2] Antibiotic resistance group, Max Planck Institute for Evolutionary Biology, Ploen, Schleswig-Holstein, Germany

[3] Evolutionary Ecology and Genetics, Zoological Institute, Kiel University, Kiel, Schleswig-Holstein, Germany

*Shared first authorship with an interchangeable order

[$]Senior and corresponding author: c.kaleta@iem.uni-kiel.de

Georgios Marinos ORCID 0000-0002-6443-7696

Johannes Zimmermann ORCID 0000-0002-5041-1954

Jan Taubenheim ORCID 0000-0001-7283-1768

Christoph Kaleta ORCID 0000-0001-8004-9514

1. Abstract

Host-microbial metabolic interactions have been recognised as an essential factor in host health and disease. Genome-scale metabolic modelling approaches have made important contributions to our understanding of the interactions in such communities. One particular such modelling approach is BacArena in which metabolic models grow, reproduce, and interact as independent agents in a spatiotemporal metabolic environment. Here, we present a modelling application of BacArena, a virtual colonic environment, which reveals spatiotemporal metabolic interactions in a computational colonic environment. This environment resembles the crypt space together with the mucus layers, the lumen and fluid dynamics. Our proof-of-principle experiments include mono-colonisation simulations of context-specific colonic cells and simulations of context-specific colonic cells with the SIHUMIx minimal model microbiome. Our simulations propose host-microbial and microbial-microbial interactions that can be verified based on the literature. Most importantly, the Virtual Colon offers visualisation of interactions through time and space, adding another dimension to the genome-scale metabolic modelling approaches. Lastly, like BacArena, it is freely available and can be easily adapted to model other spatially structured environments (http://www.github.com/maringos/VirtualColon).

2. Introduction

Host-microbial interactions are of crucial importance for host health and fitness[1]. A well-studied example of localised host-bacterial interactions is the mammalian large intestine, where the gut microbiome provides the host with nutrients that otherwise would not be available to the host, protects it from colonisation by pathogens and interacts with its immune and nervous system[2]. For instance, some colonic bacteria can ferment fibres and other components in the colonic lumen. Subsequently, they produce short-chain fatty acids (SCFAs), such as acetate, butyrate and propionate that have diverse beneficial properties for host health[3,4]. Acetate and propionate are carried and utilised metabolically outside the intestine[5], while butyrate is used locally for energy generation[6]. However, their effect on the host is not only metabolic, as there is evidence of an interaction between SCFA and the immune system[7].

However, the case of SCFA is far from exceptional[8]. Therefore, it would be very informative to systematically explore host-microbial interactions inside the colonic microenvironment. In the colon, bacteria reside and are separated from the colonic tissue by two layers of a host-produced mixture of glycoprotein and oligosaccharides, collectively called mucus, which is located in between the lumen and the colonic epithelium[9]. This environment is characterised by the limited presence of oxygen fostering the growth of anaerobic bacteria under physiological conditions[10,11]. The bacteria consume dietary compounds that are not absorbed in the small intestine along with host-derived compounds such as mucus and bile[12]. Therefore, it is not surprising that the architecture of the colonic micro-environment offers a palette of well-studied localised host-bacterial interactions, as well as unknown ones.

Attempts to model this physicochemical environment and its phenomena in the intestine exist and are informative. For instance, Cremer and colleagues developed a mathematical, quantitative model that combines the microbes, their production of SCFA and colonic water absorption.[13]. However, a promising method to understand novel, unexplored host-microbial interactions is the modelling of the metabolism of both host and bacterial cells.

Recent progress in the field of Systems Biology has enabled the creation of models of metabolism for a variety of organisms. Specifically, starting from the genomic information of individual species[14,15], it is possible to infer the possible metabolic pathways of the respective organisms and to organise them in networks of interconnected metabolic reactions, known as genome-scale metabolic models[16]. As a further step, we can apply mathematical methods, such as linear programming, to simulate the input and output of these networks. A common mathematical approach is flux balance analysis (FBA), which optimises the input and output of the models so that an objective function such as cell growth is maximised[17].

Simple metabolic models, such as the *Escherichia coli* core model with less than a hundred reactions, can be used to understand how the central metabolism of an organism operates[18]. For more advanced research, one can utilise existing curated models (e.g., the extensive, human-associated bacterial models collection AGORA2[19]) or even create own models tailored to the respective research question by employing modelling software such as gapseq and CarveMe[15,20]. Most importantly, it is possible to extend the layers of knowledge by combining datasets from different omics and databases, also beyond the strict boundaries of genome-scale metabolic modelling (e.g, see Virtual Metabolic Human database[21], MetaNetX[22–25], KEGG[26–28]). Emanating from this basis, spatiotemporal approaches that focus on simulating not only the models but also their environment through time have been developed[29]. For instance, an advanced approach by Versluis and colleagues has simulated how the metabolism of specific gut bacteria could alter based on the changes of the environment cues[30].

In this study, we build on the metabolic modelling software BacArena, which is an agent-based framework for spatial and temporal simulations of metabolic models. Specifically, it allows the design of a chemically defined environment, where the cells acting as agents can have predefined properties (e.g., speed, chemotaxis, linear or exponential growth etc.)[16,31]. We present a virtual colon-like 2D and context-specific application of BacArena that combines the host and bacterial sides into one single simulation framework. Our implementation spatially separates bacteria and host cells by representing multiple mucus layers. Furthermore, it enables a realistic simulation of host and microbial interactions, as it combines spatial-dependent diffusion phenomena that constrain substrate availability and mimic the lumen faecal stream powered by peristalsis activity. Lastly, our Virtual Colon software is freely available on GitHub so that it can easily be adapted by future users (http://www.github.com/maringos/VirtualColon).

3. Material and methods

General setup

We conducted computational colonisation experiments mimicking an experimental setting with germ-free mice originally described by Geva-Zatorsky and colleagues (henceforward the reference study)[32]. Therefore, each simulation comprised bacterial models together with host models in our colon-like in-silico setting. Furthermore, each setting simulates seven iterations of one hour. The first iteration was used for the diffusion of compounds into the environment. In total, each setting was replicated ten times. The growth of each organism was calculated based on parsimonious flux balance analysis[33]. The majority of colonisation experiments referred to the introduction of one species (henceforward mono-colonisation). There were also three cases of specific-pathogen-free mice (SPF). In that case,

we employed the generic simplified human intestinal bacterial community of eight species (see Table 1, SIHUMIx)[34].

Metabolic models

In the case of the mono-colonisation experiments, bacterial metabolic models matching the bacterial strains of the reference study were used (see S1 Table)[32]. If a genome of a strain was not available, we took the most similar genome from NCBI and literature (see S1 Table) [35]. The genomes were utilised to create the respective bacterial metabolic models by gapseq[15]. The medium for gap filling was the one available in the lumen and mucus layers of the Virtual Colon (see S1 Table). The SIHUMIx metabolic models were reconstructed using gapseq[15] based on the published genomic information by Becker and colleagues[34]. The gap-filling medium was predicted by gapseq. Finally, the models were adapted to grow on the medium available in the lumen and mucus layers of the Virtual Colon. To minimise the possibility of bacterial models competing for nutritional resources with the human models, we introduced a new "d" compartment into the bacterial models to account for an exclusive nutritional uptake of compounds from the lumen.

The host metabolic models originate from an adapted version of the published Recon 2.2 model[36]. This generic model was expanded so that a new compartment of exchange reactions was available. This compartment contains exchange reactions ending with “u” and is a copy of the original compartment of exchange reactions labelled “e”. The reason for this addition was to represent the flow of compounds between the bacteria in the lumen and the colonic cells (compartment “e”) and between the colonic cells and the blood compartment (compartment “u”), following the strategy of Sahoo and Thelie[37]. Moreover, we used iMAT to integrate human transcriptomic data from the reference study[32,38] into the host models[39] to build context-specific models of the respective colonic tissue. After translating gene expression activity into reaction expression, a reaction was assumed to be lowly expressed if it was within the first quartile of all reaction expression values. A reaction was assumed to be highly expressed if it was in the fourth quartile across all reaction expression values Moreover, we required a pre-set list of forced reactions and unconstrained nutrition-related exchange reactions. This information was used as input to determine a context-specific model for each condition. All exchange reactions and the demand reaction for ATP “DM atp c” were available in the final models. Detailed information on the utilised models and the procedures can be obtained from Table 1 and the models are available online (see S1 Table and supplementary folder ‘Models’).

Representation of the colon

The computational space of the Virtual Colon was developed by extending BacArena, which provides a two-dimensional grid area[31]. One bacterial or host cell was located in one grid cell. The size of the Virtual Colonic lumen, the mucus layers, and the structure of the colonic crypts were calculated based on anatomic measurements converted to the dimensions of one grid cell. Specifically, thanks to a predefined crypt-like position of the host cells in the environment, two half-crypts were represented together with their common inter-cryptal space (see Fig. 1 and Table 1).

The mucus layers and the lumen of the Virtual Colon were located on top of the crypts, while below the crypts an area representing the submucosal space and the bloodstream was

added. The inner mucus' width was equal to one-third of the total mucus one, while the outer mucus' width was equal to two-thirds[40]. The concentration of outer mucus layer compounds was found to be four times greater than that of the outer ones[41] and was used accordingly (see S2 Table for more information on design, calculation, and further references). The bacterial models were introduced in the colonic lumen and both mucus layers. The bacteria of the inner mucus were unable to move unless the inner mucus was partially degraded. To this end, in each simulation step, the molecular quantities of inner mucus compounds were checked. If the amount of at least one compound around a grid cell of the inner mucus layer was equal to or less than the quantity of the outer layer, then the bacterial models could move through the grid cell and pass towards the host. The bacterial models could not enter human space, but they could be located next to the human models.

We started the simulations with reported abundances from the reference study [32]. The initial position of microbial cells in the Virtual Colon was random. Important additional parameters were: the arena's size and volume, the actual total volume of the murine host's caecum, colon and rectum (0.37 cm^3)[42], the bacterial input (200µl of 10^8 cfu/ml; personal communication with Kasper Dennis ((dennis_kasper@hms.harvard.edu), correspondent author of the reference study[32]). For instance, the amount of bacteria in the lumen was calculated based on these formulas:

$$Amount_{lumen} = \frac{Area_{lumen} * Volume_{arena} * 0.2 * 10^8}{Area_{total}}$$

$$Volume_{arena} = Length_{Xaxis} * Length_{Yaxis} * \sqrt{Length_{Xaxis} * Length_{Yaxis}}$$

Similarly, the amount of bacteria in the outer and inner mucus areas was calculated. In the case of the SIHUMIx community simulations, the same approach was followed. However, an abundance factor accounting for the relative abundances of each species was used (see Table 1).[34]

The virtual host cells inherited the default human class settings of BacArena[31]. For the minimum weight and its standard deviation, the scaling factor was used to relate the area of human and bacterial cells. Rodriguez and colleagues have suggested that one crypt column is as long as 31.1 cells in the descending mouse colon [43]. Similarly, the two-crypt setting provided 70 model slots for host cells in total. Since the maximum allowed weight of 70 cells represented a maximum total weight of around all cells of a human crypt (BNID 110648 [44]). In addition to these adjustments, no movement was allowed for the models, and their growth was considered to be linear through time (see Table 1). It should be noted that while there is some debate about whether optimisation of growth is an adequate objective function for flux balance simulations of colonic cells, the biomass function includes all molecular components of cells also required for cell renewal. Furthermore, there is constant growth and shedding of colonic cells with an estimated turnover time of 3-5 days in mice[45]. Thus, in the colonic context, optimisation of growth is a valid objective function to predict metabolic fluxes.

The transport of molecules inside BacArena [31] was modelled by diffusion (see S2 Table). The arena was split into the following diffusion sectors: lumen, outer mucus layer, inner mucus layer, intermediate layer in-between, and blood. The utilised diffusion coefficients were calculated using a power regression function (coefficients vs. molecular weight) for the colonic lumen and mucus layers. The molecular weight was used for nutritional compounds. For other compounds, the default value of glucose was assumed. The regression functions were generated using the intestinal diffusion data of Winne and colleagues [46]. The same strategy

was followed for the restricted areas and the lumen [47]. Especially for mucus layers, the diffusion coefficients of molecules in outer mucus were equal to ⅔ of mucus diffusion coefficients, while for inner mucus, they were equal to ⅓ of mucus diffusion coefficients, based on the observation that ⅓ of the length of the mucus belongs to the inner layer [40]. Furthermore, the mucus compounds were not allowed to diffuse to represent the stability of the mucus in the colonic environment. Oxygen could only diffuse to host areas to ensure limited "oxygenation" of the Virtual Colon. Practically, the diffusion of compounds in the lumen was designed to be less restricted than in mucus layers, while not possible in the intermediate layer and in blood. At the same time, diffusion of blood molecules was possible in the intermediate layer and in the blood.

Nutrition

Following the nutrition that was chosen by the authors of the reference publication [32], the primary source of nutritional compounds was the LabDiet ® JL Rat and Mouse/Auto 6F 5K67. These compounds were matched to the dietary bacterial exchange reactions to exclude nutritional competition between host and bacterial cells. The intestinal absorption and the dimensions of the Virtual Colon were considered for calculating the exact nutritional input. In addition, some components such as water, H^+, minerals, vitamins, and mucus compounds were added as part of the lumen compartment. To represent the inflow of nutrients from the blood circulation, a minimal collection of compounds was added into the blood compartment. Their concentration was based on the literature (e.g., (BNID 110365 [44]) and various Human Metabolome Database entries (https://hmdb.ca/ [48–51]). To infer these components, a shadow cost analysis based on the BacArena [31] function "plotShadowCost" was utilised (see supplementary folder 'Definition_Blood'). A list of compounds can be found in the S2 Table.

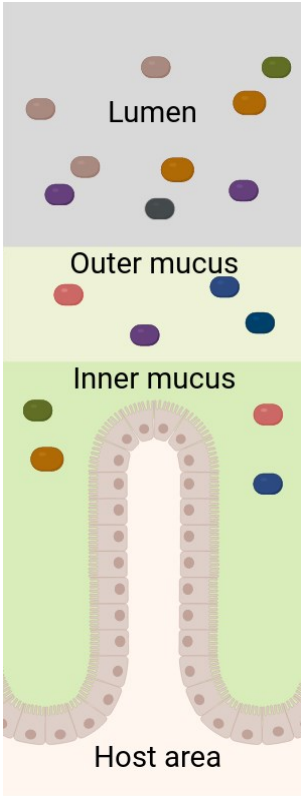

Figure 1: Schematic representation of the virtual colonic space. The coloured rectangles represent the models of the microbial species and the two shades of green represent the two mucus layers above the host's epithelium. Created with BioRender.com.

Table 1: Overview of properties of the Virtual Colon

Property	Information on values & units	Further comments	Reference
Grid cell dimension	0.00025 × 0.00025 cm^2	Default in BacArena	[31]
Y-axis size	179-grid-cell-long	Set by the developers	Not applicable
X-axis size	24-grid cell-long	Set by the developers	NA
Scaling factor for minimum weight and its standard deviation of host models	$\frac{132.73229}{4.42}$	A human COLO205 colon cell has a diameter of 13 µm; hence its area is equal to 132.73229 μm^2. The area of a bacterium in BacArena is, by default, 4.42 μm^2.	[44] BNID 108890
Scaling factor for maximum weight of host models	$\frac{1000}{70}$	70 cells represent the weight of around 1000 cells of a human crypt	[43,44] BNID 110648[44]
Starting amount of bacteria in the lumen	29	Set by the developers	Not applicable
Starting amount of bacteria in the outer mucus	18	Set by the developers	Not applicable
Starting amount of bacteria in the inner mucus	9	Set by the developers	Not applicable
Relative abundance of *Anaerostipes caccae* in SIHUMIx simulations	0.1263867	Based on the concentration in human faeces [log10 cells / g dry matter]; see text	[34]
Relative abundance of *Bacteroides thetaiotaomicron* in SIHUMIx simulations	0.1444797	Based on the concentration in human faeces [log10 cells / g dry matter]; see text	[34]
Relative abundance of *Bifidobacterium longum* in SIHUMIx simulations	0.1388008	Based on the concentration in human faeces [log10 cells / g dry matter]; see text	[34]
Relative abundance of *Blautia producta* in SIHUMIx simulations	0.1385367	Based on the concentration in human faeces [log10 cells / g dry matter]; see text	[34]
Relative abundance of *Clostridium butyricum* in SIHUMIx simulations	0.1065769	Based on the concentration in human faeces [log10 cells / g dry matter]; see text	[34]
Relative abundance of *Clostridium ramosum* in SIHUMIx simulations	0.1263867	Based on the concentration in human faeces [log10 cells / g dry matter]	[34]
Relative abundance of *Escherichia coli* in SIHUMIx simulations	0.118859	Based on the concentration in human faeces [log10 cells / g dry matter]	[34]
Relative abundance of *Lactobacillus plantarum* in	0.09997359	Based on the concentration in human faeces [log10 cells / g dry	[34]

SIHUMIx simulations		matter]	

Software

The simulations and analyses thereafter presented in this manuscript were conducted in the R environment (version 4.2.1) [52]. Optimisations were generally conducted using the BacArena application (version 1.8.2, commit euba/BacArena@dc8e591 and euba/BacArena@008d186) [31] and sybil (version 2.2.1, commit SysBioChalmers/sybil@58eb989) [53]. The linear programming solver was CPLEX (academic version 22.1.0) [54], which is available through the R package cplexAPI (version 1.4.0) [55]. For data management, the software tidyverse (version 2.0.0) [56] and especially its library dplyr (version 1.1.4) [57] were used. For plotting, the software ggplot2 (version 3.5.1) [58], ggvenn (version 0.1.10)[59], ggthemes (version 5.1.0) [60], scales (version 1.3.0) [61], ggalluvial (version 0.12.5) [62], and BacArena (version 1.8.2, commit euba/BacArena@dc8e591) [31] were utilised. The software devtools (version 2.4.5) [63] was also used to manage the R environment.

4. Results

The main objective of this study was to provide a computational framework to simulate host-microbial interactions in the mammalian colon. We first used our approach to study host-microbiome interactions in the colon based on a previously published dataset of single-strain colonisation experiments in germ-free mice[32]. Besides microbial abundance data, Geva-Zatorsky and colleagues provided extensive transcriptomic datasets of these colonisation experiments. Based on those transcriptomes, we reconstructed context-specific models of colonic tissue for the respective mice. For our study, we used context-specific Recon 2.2 [36] host models along with bacterial models for joint simulations in a virtual colon.

The Virtual Colon provides detailed information on the host-microbial metabolic interactions in space and time. To reveal those interactions in the mono-colonisation experiments, we extracted all fluxes across all time points for each compound and for each model. Since a positive flux shows production and a negative one shows consumption of a compound, we calculated the sum of fluxes of all models for each compound. Collectively, the host models produced 20 compounds and the bacterial ones produced 27 compounds (Fig. 2A). Interestingly, the host-microbial interactions seem to be very pair-specific, since we could identify compounds that in some pairs are bacterially produced or in other pairs by the host (eg., glycine, L-alanine; Fig. 2A). Furthermore, we observed the host exchange of nitrogen-containing compounds, towards the bacterial models, and the uptake of bacterially produced SCFA. Additionally, we found that although the majority of the bacteria interacted metabolically with the host regardless of their position (e.g., see cases with fluxes of models originated from all three layers: lumen, outer mucus, inner mucus, Fig. 2B), we also observed cases of localised interactions (Fig. 2B).

Further, we employed the Virtual Colon to study host-bacterial interactions with the SIHUMIx bacterial community. Fig. 3A shows how the SIHUMIx microbial community that resides in inner and outer colonic mucus gradually consumed the mucus compound N-acetylneuraminate. Furthermore, the bacteria inside the inner mucus layer could only marginally spread in comparison to the other positions due to the design movement barrier. Most interestingly, the decreasing quantity of those compounds follows the growth of the

293 bacteria models in the area. The bacterial models of *Bacteroides thetaiotaomicron*, *Blautia*
294 *producta*, and *Clostridium butyricum* can degrade N-acetylneuraminate (Fig. 3B).

295 The observation of microbial mucus degradation led to more general questions on what
296 compounds are consumed or produced by the metabolic models. The host models, similarly
297 to the mono-colonisation experiments, are context-specific Recon 2.2 models[36], whose
298 reconstruction was based on the transcriptomes GSM2354402, GSM2354403 and
299 GSM2354404 respectively. While those three models produce and consume mostly the same
300 compounds, they do have distinct metabolic profiles that can be attributed to the different
301 transcriptomes. For instance, the recon model GSM2354403 produced L-alanine, which was
302 taken up by the bacteria, while the recon model GSM2354404 consumed bacterial L-alanine
303 (Fig. 4A and 4D). However, all models consumed bacterially produced short-chain fatty acids,
304 such as formate, acetate, propionate, and butyrate (Fig. 4C and 4D). Interestingly, the models
305 exchange various metabolic compounds (e.g., water, vitamins, amino acids, TCA-cycle
306 compounds such as alpha-oxoglutarate).

307 Not only were the bacterially produced compounds taken up by the host models, but
308 they were also consumed by other bacterial species of the community (Fig. 5A and 5B). For
309 instance, apart from amino acids and carbon sources, they also exchanged metabolites like
310 protons, ammonium, phosphate, and hydrogen sulphide. It is possible to characterise the
311 metabolic role of community members. The bacteria model of *E. coli* was the most active
312 species in terms of production and consumption of compounds. On the other hand, *B. longum*
313 and *C. butyricum* contributed more compounds than they consumed, while the opposite was
314 true for *A. caccae* and *B. producta*.

315 Furthermore, in order to understand how the metabolic interactions change when
316 comparing the interactions from mono-colonisation with the SIHUMIx simulations, we
317 investigated which compounds are unique in each of the two settings. It can be observed that
318 the exchanged compounds were mostly common (Fig. 6). However, the majority of the unique
319 compounds in mono-colonisation experiments were nitrogen-containing compounds. In the
320 other two parts of the Venn diagram, we could identify amino acids, metabolism intermediates
321 (e.g. fumarate) and short-chain fatty acids.

322

323

324

325

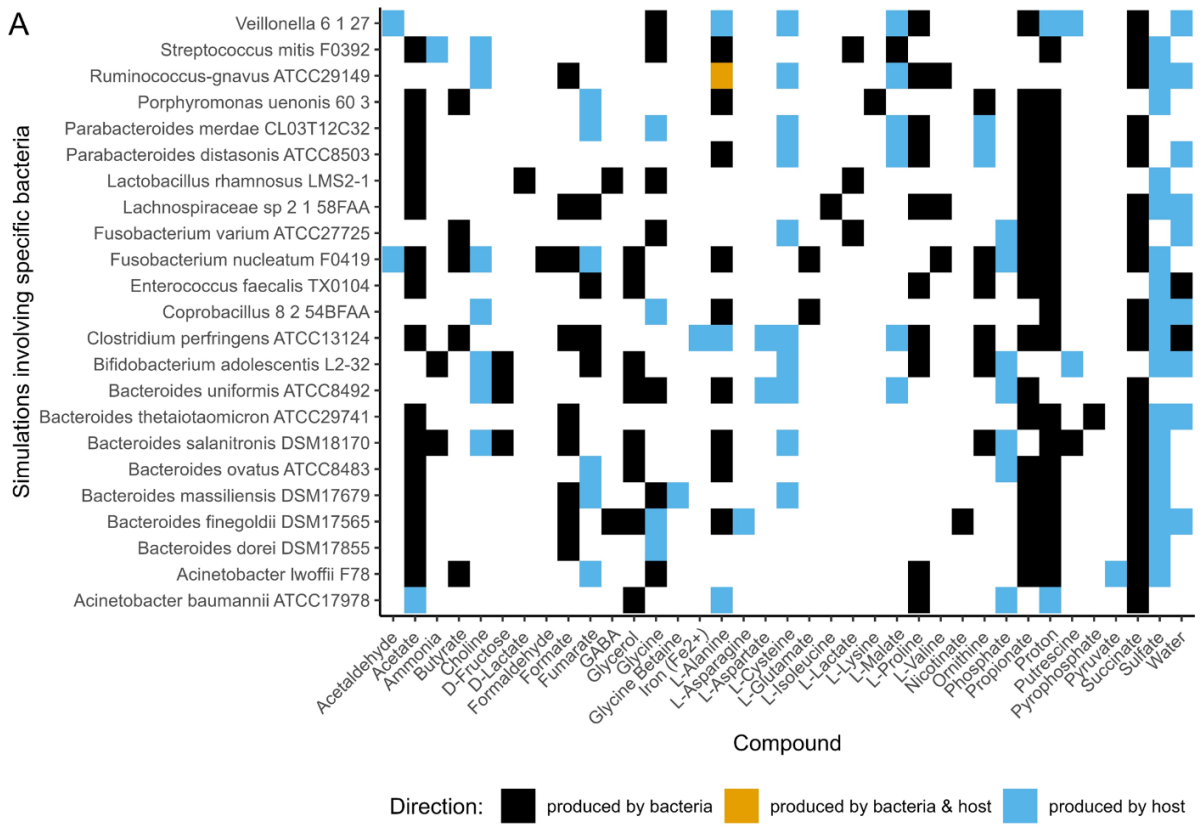
A
Simulations involving specific bacteria
Veillonella 6 1 27
Streptococcus mitis F0392
Ruminococcus-gnavus ATCC29149
Porphyromonas uenonis 60 3
Parabacteroides merdae CL03T12C32
Parabacteroides distasonis ATCC8503
Lactobacillus rhamnosus LMS2-1
Lachnospiraceae sp 2 1 58FAA
Fusobacterium varium ATCC27725
Fusobacterium nucleatum F0419
Enterococcus faecalis TX0104
Coprobacillus 8 2 54BFAA
Clostridium perfringens ATCC13124
Bifidobacterium adolescentis L2-32
Bacteroides uniformis ATCC8492
Bacteroides thetaiotaomicron ATCC29741
Bacteroides salanitronis DSM18170
Bacteroides ovatus ATCC8483
Bacteroides massiliensis DSM17679
Bacteroides finegoldii DSM17565
Bacteroides dorei DSM17855
Acinetobacter lwoffii F78
Acinetobacter baumannii ATCC17978
Acetaldehyde
Acetate
Ammonia
Butyrate
Choline
D-Fructose
D-Lactate
Formaldehyde
Formate
Fumarate
GABA
Glycerol
Glycine
Glycine Betaine
Iron (Fe2+)
L-Alanine
L-Asparagine
L-Aspartate
L-Cysteine
L-Glutamate
L-Isoleucine
L-Lactate
L-Lysine
L-Malate
L-Proline
L-Valine
Nicotinate
Ornithine
Phosphate
Propionate
Proton
Putrescine
Pyrophosphate
Pyruvate
Succinate
Sulfate
Water
Compound
Direction:
produced by bacteria
produced by bacteria & host
produced by host

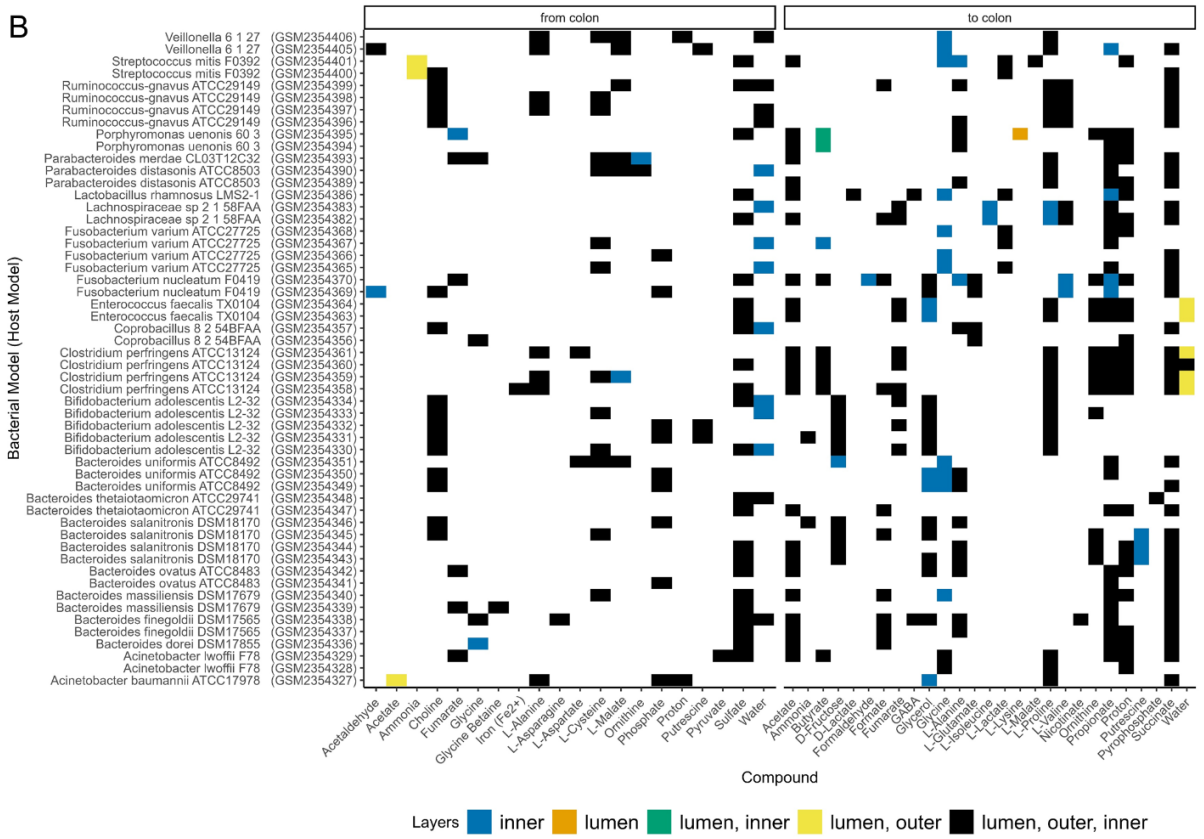
B
from colon
to colon
Bacterial Model (Host Model)
Compound
Layers
inner
lumen
lumen, inner
lumen, outer
lumen, outer, inner

Figure 2: A. Exchange of compounds which are produced by the bacterial models or context-specific host models. The colour of the layers depends on the origin of the producer. B. Exchange of compounds which are produced by the host models and are consumed by the bacterial model and vice versa. To estimate the exchange of compounds among the models, the sum of all fluxes across time for each compound and for each model was determined. A positive sum denotes production, while a negative one denotes consumption. To limit the numerical artefacts, the fluxes whose absolute value was less than 1E-6 were considered zero.

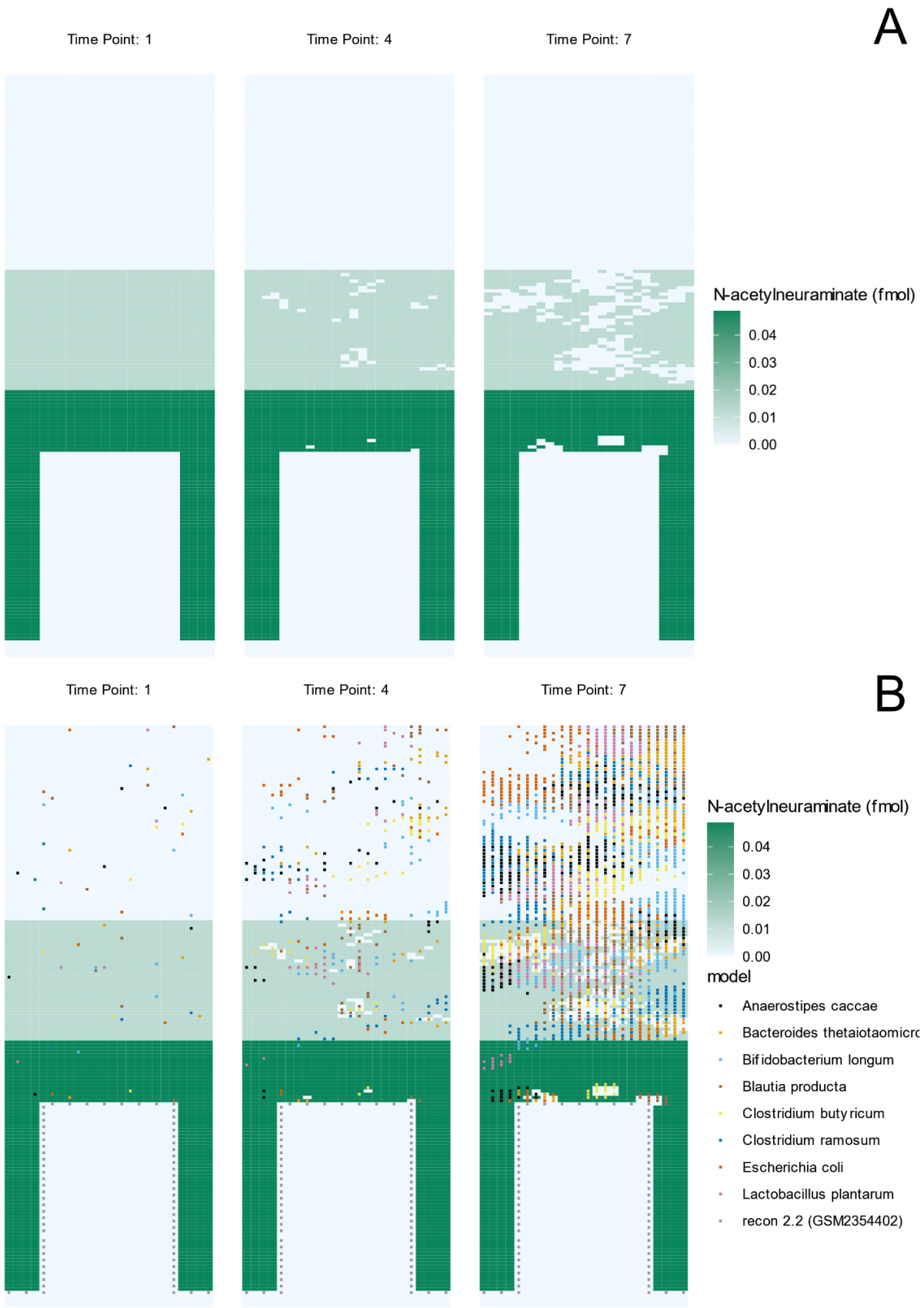

Figure 3: A. Schematic representation of the mucus compound N-acetylneuraminate through three-time points in a SIHUMIx-host simulation (GSM2354402, 10th replicate) B. Same as A

with the inclusion of the SIHUMIx bacterial species. Each subplot represents the substance concentration and bacterial population per time point in hours.

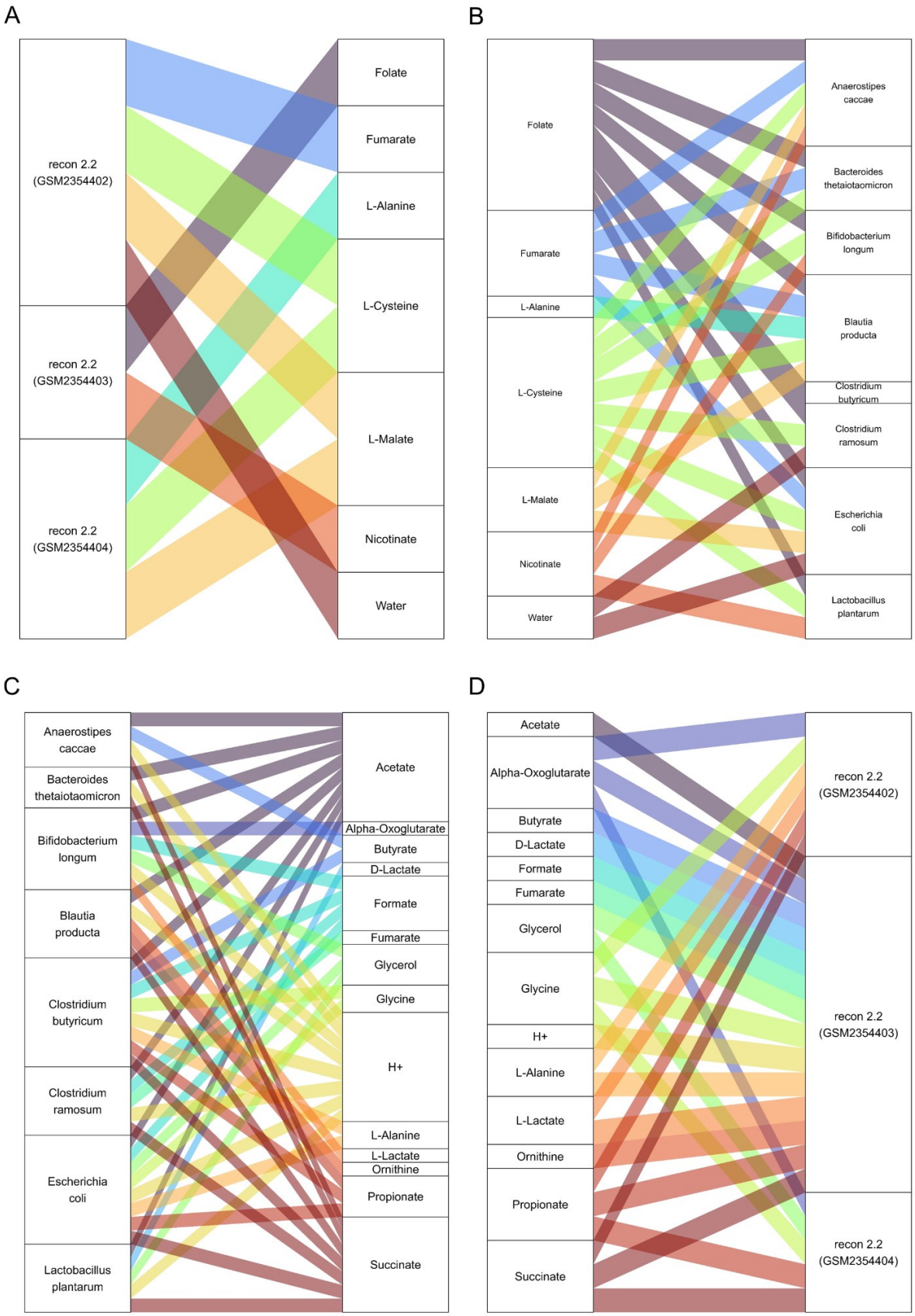

Figure 4: Schematic representation of compounds produced by the context-specific host models (A) and consumed by the SIHUMIx bacteria (B) along with the bacterially produced

ones (C) that are consumed by the host models (D). Metabolites with the highest interaction frequency (>= 50%) across all time points and simulations were selected to be plotted for simplicity. For the full dataset, see S3 Table.

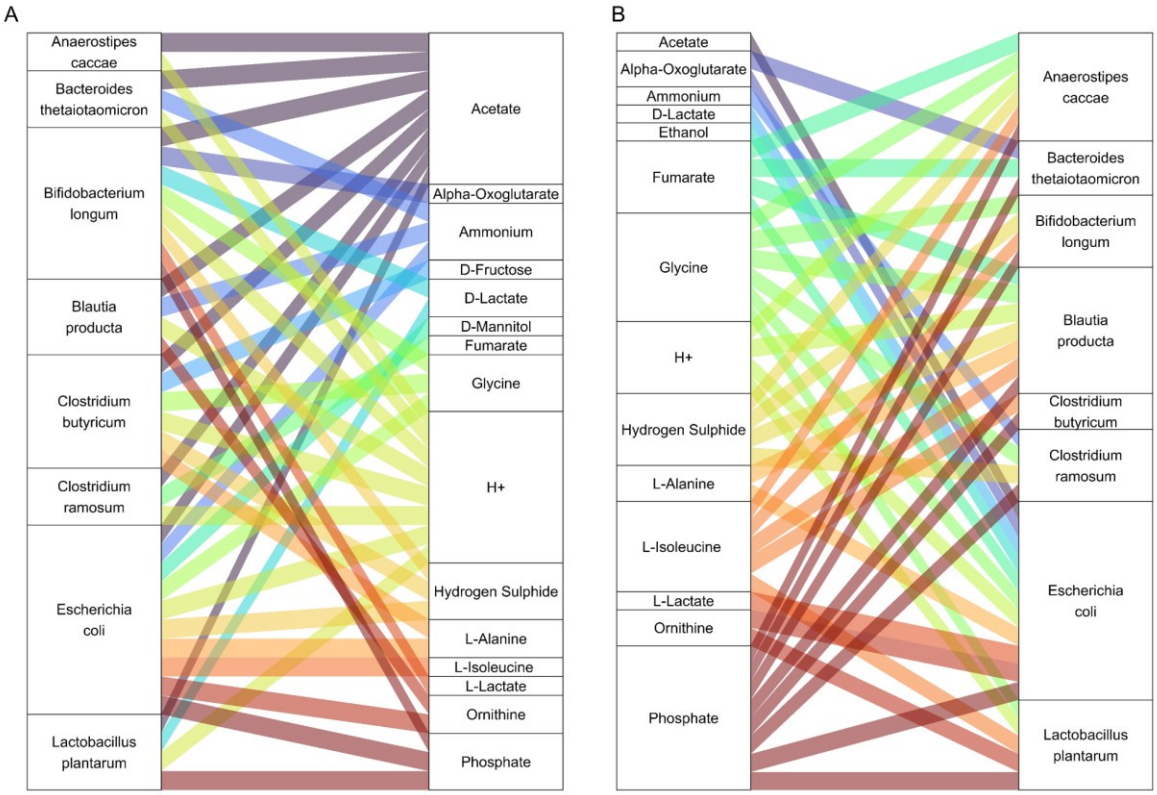

Figure 5: Schematic representation of compounds produced by the SIHUMIx bacterial models (A) and consumed by other SIHUMIx bacterial models (B). Metabolites with the highest interaction frequency (>= 50%) across all time points and simulations were selected to be plotted for simplicity. For the full dataset, see S3 Table.

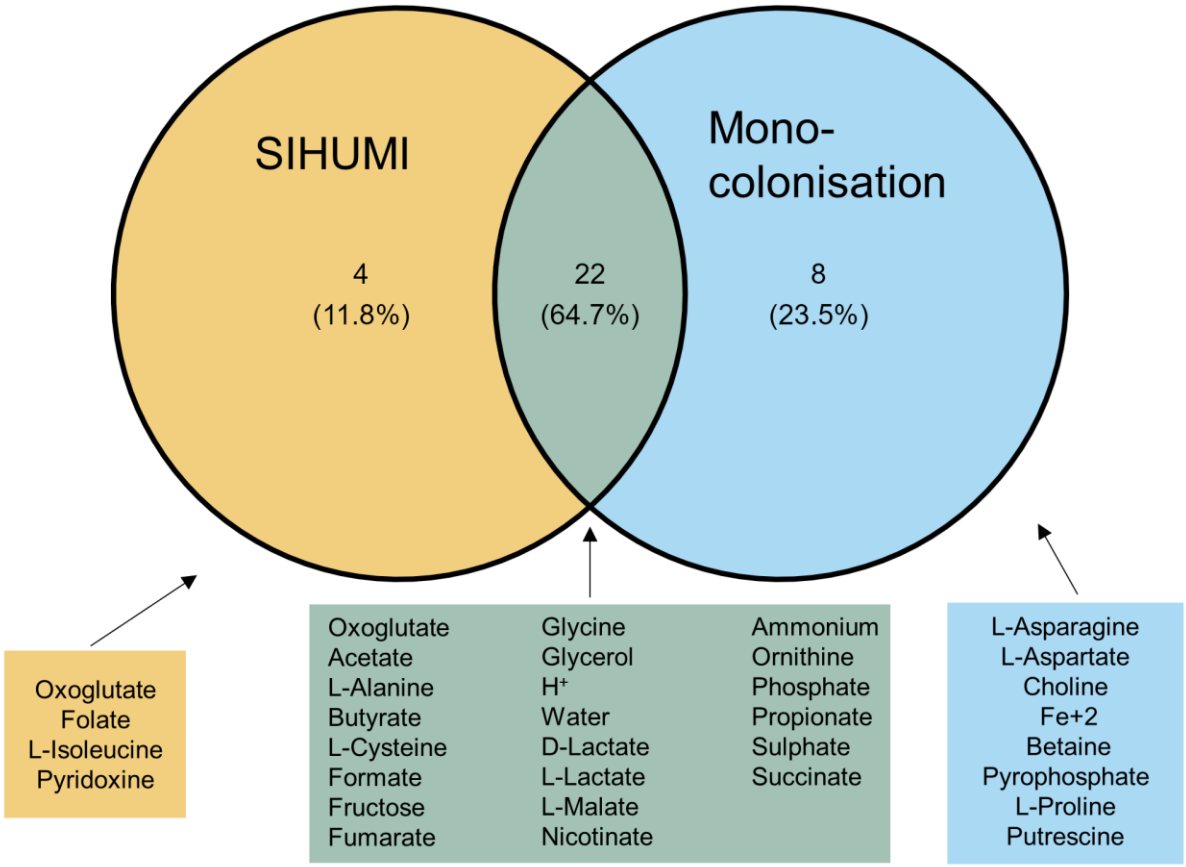

Figure 6: Schematic representation of compounds exchanged by the bacterial models and host models in the mono-colonisation and SIHUMIx experiments. Only interactions with bacteria from the shared genera were taken into account (Bacteroides, Bifidobacterium, Clostridium, Lactobacillus). All simulation time points were included in the analysis.

Table 2: Comparison of Virtual Colon with other published approaches

Name	Approach	Microbes	Scope	Host	Space	Time	Mucus	Gut motility	Availability	Reference
Gut-Microbiota	PDE model with fluid dynamics (Stokes)	Movement + predefined functions	Colon	Nutrient uptake	✓	✓	✓	✓	Matlab code https://forgemia.inra.fr/simon.labarthe/gut-microbiota	64
MicroGutPop	ODE model (Monod equation)	predefined functional groups	Colon	-	-	✓	✓	✓	R package https://github.com/HelenKettle/microPopGutCode	65
GutLogo	ABM		Ileum	-	✓	✓	✓	✓	https://github.com/GutLogo/GutLogo	66
Synthetic Gut Microbiome	ODE model (gLV)	25 microbes	Butyrate production	-	-	✓	-	-	Julia code https://github.com/RyanLincolnClark/DesignSyntheticGutMicrobiomeAssemblyFunction	67
Virtual Colon	ABM + PDE	Movement + metabolic model	Colon	Metabolic model	✓	✓	✓	✓	R code http://www.github.com/maringos/VirtualColon	this article

PDE: Partial differential equation; ODE: Ordinary differential equations; gLV: generalised Lotka-Volterra; ABM: Agent-based modelling

5. Discussion

Host-bacterial metabolic interactions are considered important drivers of host health and fitness. Therefore, one of the objectives of this study was to develop a data-driven approach that allows us to systematically explore the compounds that are exchanged between the host and bacterial cells. Here we present the Virtual Colon that extends the agent-based modelling framework BacArena[16,31] to study host-microbiome interactions in the mammalian large intestine. Specifically, it enables host-microbial simulations, in which bacteria and host cells are spatially separated through multilayer mucus layers. Moreover, it includes spatial-dependent diffusion that constrains substrate availability for the models. Most importantly, it not only enables the joint simulation of host and microbial interactions but also visualises them. While other methods have contributed to the field either by using differential equations and/or

agent-based modelling (Table 2), the Virtual Colon, which is built on BacArena, combines them in one software framework.

In our simulations, we utilised host models that originated from the human model Recon 2.2[36]. For the simulations, the host models were adapted using transcriptomic data[38] from mono-colonisation experiments of germ-free mice with the respective species[32]. In the case of colonisation with non-specific pathogens, we used the SIHUMIx bacterial models that comprise a generic eight-species human intestinal bacterial community[34].

To continue with the host-bacterial interactions in the mono-colonisation experiments, the observed usage of cysteine by some bacteria of the genus *Fusobacterium* and *Clostridium* is in line with the literature, which proposes that cysteine is metabolised by bacteria, leading to hydrogen sulphide[68]. Hydrogen sulphide has been characterised as a compound with multiple effects, as in low levels, it supports colonic health, while in excess, it is associated with inflammatory and pathological states (e.g., inflammatory bowel disease and cancer)[68].

Additionally, the compound 4-aminobutanoate, also known as γ-aminobutyric acid (GABA), is predicted to be produced by *Lactobacillus rhamnosus* and *Bacteroides finegoldi* and be consumed by the host models, which is in accordance with the literature[69]. This compound may act on the central nervous system as well as the enteric nervous system of the host as part of the microbiota-gut-brain axis[69]. On the other hand, *Bacteroides finegoldi* has not been reported to be a GABA producer. However, a recent article proposed that the Bacteroides species can produce this molecule, although, in the simulations, no other *Bacteroides* species did so[70].

Recently, a study based on metabolomics focusing on the colonic absorption of compounds with low molecular weight in mice identified some of the computationally predicted compounds, which were subject to metabolic exchange in our simulations: (glycine) betaine, cholinem, alanine, glutamine, glycine, isoleucine, lactate, ornithine, and short-chain fatty acids (Fig. 2A, B) [71]. Interestingly, host-derived glycine betaine and choline can be further bacterially metabolised to trimethylamine-N-oxide and trimethylamine, for which a linkage to atherosclerotic cardiovascular disease has been demonstrated[72].

While mono-colonisation experiments offered a detailed overview of pairwise host-bacterial interactions, the bacterial species found in the mammalian colon are quite diverse. Therefore, we selected the representative SIHUMIx community to investigate how our results change in the context of a more complex community. Our simulations showed a wide exchange of compounds among the species as well as between bacteria and host cells. Not surprisingly, many byproducts were found also in mono-colonisations, implying that the repertoire of metabolic exchanges may be genera-dependent (Fig 6). The bacterial models create a complex web of compounds, where carbohydrate and amino acid metabolism as well as cofactors (e.g. vitamins) and byproducts are the most common end products. This observation becomes intriguing, if one considers that carbohydrates rather than amino acids are primarily used in bacterial energy metabolism, as amino acid metabolism is less cost-effective[73]. Moreover, this finding suggests that mono-colonisation experiments only partially capture interactions that can be observed in community colonisation, as the metabolic repertoire and signature may alter significantly.

It must be stated that the predicted exchange of compounds between the host and the bacterial models is based on the assumption that the host colonic cells can exchange compounds from the luminal side of the colon. For instance, amino acids are known to be absorbed in the small intestine, while their absorption fate in the large intestine is unclear.

While the colonic bacteria can metabolise the remaining amino acids, it is proposed that some of them can be used by colonocytes [74]. In parallel, it has been shown that colonocytes can excrete amino acids (e.g., alanine, aspartate, asparagine, isoleucine, and valine) in both apical and basolateral directions in vitro [75]. Therefore, the observed production or consumption of several compounds by the host is feasible and waits for further experimental validation. These experiments should investigate the transport of metabolites across the intestinal barrier. Such a pivotal set of experiments was performed by Li and colleagues, who identified gut species that deplete and metabolise amino acids throughout the intestine and therefore regulate host metabolism [76].

Furthermore, the Virtual Colon includes spatial parameters tailored to the large intestinal environment. For instance, the diffusion of compounds inside the mucus layer is limited and the bacteria in the inner mucus cannot move unless mucus is consumed by community members, such as *B. thetaiotaomicron*, a known mucus-degrading species [77](Fig 3). Additionally, our results proposed that there are spatial, localised interactions, therefore it could be suggested that the mucus layers can affect bacterial metabolism. (Fig 2B). Therefore, the simulation data suggests that our mucus both resembles the function of the mucus as a physical barrier and as well as a nutrient pool for the bacteria [9].

While the setting of the Virtual Colon recapitulates some of the observed host-microbial functions, there is also room for further expansions in the simulation setting. Future computational experiments may include more complex bacterial communities along with an improved representation of the abundance of bacteria with respect to the size of the simulated colon (e.g., the ratio of microbial abundance over the number of human models). Another improvement could include metabolomic data from colonic tissue and lumen so that the chemical environment is as realistic as possible. Additionally, single-cell transcriptomics would allow the representation of the various cell types of the host tissue. To improve the realism of the simulations, the Virtual Colon also has the capacity to mimic the lumen faeces stream powered by peristalsis activities, if the related parameters are set in the simulation settings. Most importantly, the presented approach provides users with an easily adaptable platform that can include all of these extensions.

In summary, our novel simulation framework, Virtual Colon, builds upon the popular BacArena platform to create a comprehensive tool for studying host-microbe interactions in the colon. By spatially separating bacteria and host cells and incorporating multilayer mucus representation, the Virtual Colon enables the realistic simulation of host-microbial interactions. This is achieved through a spatial-dependent diffusion mechanism that constrains substrate availability and accurately mimics the faecal stream. Furthermore, the Virtual Colon allows for the joint simulation of host and microbial interactions, which we demonstrated for human gut microbiome communities and personalised host models using omics data. Notably, we employed the Virtual Colon to identify species-specific mucus layer degradation and amino acid exchange between microbes and host, providing valuable insights into the intricate dynamics of the gut ecosystem. Our freely available software on GitHub invites future researchers to adapt and expand its capabilities to advance host-microbe interaction studies.

6. Authors' Contribution

Conceptualisation: GM, JZ

Methodology: GM, JZ, JT, CK

Software: GM, JZ

Formal analysis: GM
Investigation: GM, JZ, JT
Resources: CK
Data Curation: GM
Writing - Original Draft: GM, JZ
Writing - Review & Editing: All co-authors
Visualisation: GM
Supervision: CK, JZ
Project administration: GM
Funding acquisition: CK

7. Acknowledgements

CK acknowledges support from the German Research Foundation for the support through the collaborative research centre 1182 Origin and Function of Metaorganisms (sub-project A1), the research unit miTarget (FOR5042), and the excellence cluster “Precision medicine in chronic inflammation” (EXC2167) and additionally the German Ministry for Education and Research (E:Med iTREAT, support code 01ZX1902A). This research was supported in part through high-performance computing resources available at the Kiel University Computing Centre. The authors thank Dr Ahmed Samer Kadib Alban for providing them with critical opinions on the manuscript.

8. Conflict of Interest

The authors declare that they have no conflict of interest.

9. Supplementary Information

The software is freely available on GitHub (www.github.com/maringos/VirtualColon, commit: 0e56bda). The simulation RDS files that are related to this manuscript can be found on Figshare (www.doi.org/10.6084/m9.figshare.25997962). The supporting information including figures, scripts and datasets related to this manuscript can be found on Figshare (www.doi.org/10.6084/m9.figshare.25998073).

10. References

1. Ruuskanen, M. O., Sommeria-Klein, G., Havulinna, A. S., Niiranen, T. J. & Lahti, L. Modelling spatial patterns in host-associated microbial communities. *Env. Microbiol* **23**, 2374–2388 (2021).
2. Hou, K. *et al.* Microbiota in health and diseases. *Signal Transduct. Target. Ther.* **7**, 135 (2022).

515 3. Morrison, D. J. & Preston, T. Formation of short chain fatty acids by the gut microbiota
516 and their impact on human metabolism. *Gut Microbes* **7**, 189–200 (2016).
517 4. Shimizu, H. *et al.* Dietary short-chain fatty acid intake improves the hepatic metabolic
518 condition via FFAR3. *Sci Rep* **9**, 16574 (2019).
519 5. Van Treuren, W. & Dodd, D. Microbial Contribution to the Human Metabolome:
520 Implications for Health and Disease. *Annu. Rev. Pathol. Mech. Dis.* **15**, 345–369 (2020).
521 6. Donohoe, D. R. *et al.* The Microbiome and Butyrate Regulate Energy Metabolism and
522 Autophagy in the Mammalian Colon. *Cell Metab.* **13**, 517–526 (2011).
523 7. Yao, Y. *et al.* The role of short-chain fatty acids in immunity, inflammation and
524 metabolism. *Crit. Rev. Food Sci. Nutr.* **62**, 1–12 (2022).
525 8. Fogelson, K. A., Dorrestein, P. C., Zarrinpar, A. & Knight, R. The Gut Microbial Bile Acid
526 Modulation and Its Relevance to Digestive Health and Diseases. *Gastroenterology* **164**,
527 1069–1085 (2023).
528 9. Schroeder, B. O. Fight them or feed them: how the intestinal mucus layer manages the
529 gut microbiota. *Gastroenterol Rep* **7**, 3–12 (2019).
530 10. Konjar, Š., Pavšič, M. & Veldhoen, M. Regulation of Oxygen Homeostasis at the
531 Intestinal Epithelial Barrier Site. *Int J Mol Sci* **22**, (2021).
532 11. Litvak, Y., Byndloss, M. X. & Bäumler, A. J. Colonocyte metabolism shapes the gut
533 microbiota. *Science* **362**, (2018).
534 12. O'Keefe, S. J. D. Diet, microorganisms and their metabolites, and colon cancer. *Nat Rev*
535 *Gastroenterol Hepatol* **13**, 691–706 (2016).
536 13. Cremer, J., Arnoldini, M. & Hwa, T. Effect of water flow and chemical environment on
537 microbiota growth and composition in the human colon. *Proc. Natl. Acad. Sci.* **114**,
538 6438–6443 (2017).
539 14. Mendoza, S. N., Olivier, B. G., Molenaar, D. & Teusink, B. A systematic assessment of
540 current genome-scale metabolic reconstruction tools. *Genome Biol* **20**, 158 (2019).
541 15. Zimmermann, J., Kaleta, C. & Waschina, S. gapseq: informed prediction of bacterial
542 metabolic pathways and reconstruction of accurate metabolic models. *Genome Biol* **22**,

543 81 (2021).

544 16. Jansma, J. & El Aidy, S. Understanding the host-microbe interactions using metabolic
545 modeling. *Microbiome* **9**, 16 (2021).

546 17. Orth, J. D., Thiele, I. & Palsson, B. Ø. What is flux balance analysis? *Nat Biotechnol* **28**,
547 245–248 (2010).

548 18. Orth, J. D., Fleming, R. M. T. & Palsson, B. Ø. Reconstruction and Use of Microbial
549 Metabolic Networks: the Core *Escherichia coli* Metabolic Model as an Educational
550 Guide. *EcoSal Plus* **4**, 10.1128/ecosalplus.10.2.1 (2010).

551 19. Heinken, A. *et al.* Genome-scale metabolic reconstruction of 7,302 human
552 microorganisms for personalized medicine. *Nat. Biotechnol.* **41**, 1320–1331 (2023).

553 20. Machado, D., Andrejev, S., Tramontano, M. & Patil, K. R. Fast automated reconstruction
554 of genome-scale metabolic models for microbial species and communities. *Nucleic Acids*
555 *Res.* **46**, 7542–7553 (2018).

556 21. Noronha, A. *et al.* The Virtual Metabolic Human database: integrating human and gut
557 microbiome metabolism with nutrition and disease. *Nucleic Acids Res.* **47**, D614–D624
558 (2019).

559 22. Ganter, M., Bernard, T., Moretti, S., Stelling, J. & Pagni, M. MetaNetX.org: a website and
560 repository for accessing, analysing and manipulating metabolic networks. *Bioinformatics*
561 **29**, 815–816 (2013).

562 23. Bernard, T. *et al.* Reconciliation of metabolites and biochemical reactions for metabolic
563 networks. *Brief. Bioinform.* **15**, 123–135 (2014).

564 24. Moretti, S. *et al.* MetaNetX/MNXref – reconciliation of metabolites and biochemical
565 reactions to bring together genome-scale metabolic networks. *Nucleic Acids Res.* **44**,
566 D523–D526 (2016).

567 25. Moretti, S., Tran, V. D. T., Mehl, F., Ibberson, M. & Pagni, M. MetaNetX/MNXref: unified
568 namespace for metabolites and biochemical reactions in the context of metabolic
569 models. *Nucleic Acids Res.* **49**, D570–D574 (2021).

570 26. Kanehisa, M. KEGG: Kyoto Encyclopedia of Genes and Genomes. *Nucleic Acids Res.*

571 **28**, 27–30 (2000).

572 27. Kanehisa, M. Toward understanding the origin and evolution of cellular organisms.
573 *Protein Sci.* **28**, 1947–1951 (2019).

574 28. Kanehisa, M., Furumichi, M., Sato, Y., Kawashima, M. & Ishiguro-Watanabe, M. KEGG
575 for taxonomy-based analysis of pathways and genomes. *Nucleic Acids Res.* **51**, D587–
576 D592 (2023).

577 29. Scott, W. T. *et al.* A structured evaluation of genome-scale constraint-based modeling
578 tools for microbial consortia. *PLOS Comput. Biol.* **19**, e1011363 (2023).

579 30. Versluis, D. M. *et al.* A Multiscale Spatiotemporal Model Including a Switch from Aerobic
580 to Anaerobic Metabolism Reproduces Succession in the Early Infant Gut Microbiota.
581 *mSystems* **7**, e00446-22 (2022).

582 31. Bauer, E., Zimmermann, J., Baldini, F., Thiele, I. & Kaleta, C. BacArena: Individual-
583 based metabolic modeling of heterogeneous microbes in complex communities. *PLoS*
584 *Comput Biol* **13**, e1005544 (2017).

585 32. Geva-Zatorsky, N. *et al.* Mining the Human Gut Microbiota for Immunomodulatory
586 Organisms. *Cell* **168**, 928-943.e11 (2017).

587 33. Lewis, N. E. *et al.* Omic data from evolved *E. coli* are consistent with computed optimal
588 growth from genome-scale models. *Mol. Syst. Biol.* **6**, 390 (2010).

589 34. Becker, N., Kunath, J., Loh, G. & Blaut, M. Human intestinal microbiota: Characterization
590 of a simplified and stable gnotobiotic rat model. *Gut Microbes* **2**, 25–33 (2011).

591 35. Fritzenwanker, M. *et al.* Draft Genome Sequence and Complete Plasmid Sequence of
592 *Acinetobacter lwoffii* F78, an Isolate with Strong Allergy-Protective Properties. *Genome*
593 *Announc.* **4**, e00685-16 (2016).

594 36. Swainston, N. *et al.* Recon 2.2: from reconstruction to model of human metabolism.
595 *Metabolomics* **12**, 109 (2016).

596 37. Sahoo, S. & Thiele, I. Predicting the impact of diet and enzymopathies on human small
597 intestinal epithelial cells. *Hum. Mol. Genet.* **22**, 2705–2722 (2013).

598 38. Gene Expression Omnibus Accession Viewer. GSE88919.

599 39. Zur, H., Ruppin, E. & Shlomi, T. iMAT: an integrative metabolic analysis tool.
600 *Bioinformatics* **26**, 3140–3142 (2010).
601 40. Gustafsson, J. K. *et al.* An ex vivo method for studying mucus formation, properties, and
602 thickness in human colonic biopsies and mouse small and large intestinal explants. *Am.*
603 *J. Physiol.-Gastrointest. Liver Physiol.* **302**, G430–G438 (2012).
604 41. Johansson, M. E. V. *et al.* The inner of the two Muc2 mucin-dependent mucus layers in
605 colon is devoid of bacteria. *Proc. Natl. Acad. Sci.* **105**, 15064–15069 (2008).
606 42. Casteleyn, C., Rekecki, A., Van Der Aa, A., Simoens, P. & Van Den Broeck, W. Surface
607 area assessment of the murine intestinal tract as a prerequisite for oral dose translation
608 from mouse to man. *Lab. Anim.* **44**, 176–183 (2010).
609 43. De Rodriguez, M. S. B., Sunter, J. P., Watson, A. J., Wright, N. A. & Appleton, D. R. Cell
610 population kinetics in the mucosal crypts of the descending colon of the mouse.
611 *Virchows Arch. B Cell Pathol.* **29**, 351–361 (1978).
612 44. Milo, R., Jorgensen, P., Moran, U., Weber, G. & Springer, M. BioNumbers—the
613 database of key numbers in molecular and cell biology. *Nucleic Acids Res.* **38**, D750–
614 D753 (2010).
615 45. Park, J. *et al.* Promotion of Intestinal Epithelial Cell Turnover by Commensal Bacteria:
616 Role of Short-Chain Fatty Acids. *PLOS ONE* **11**, e0156334 (2016).
617 46. Winne, D. & Verheyen, W. Diffusion coefficient in native mucus gel of rat small intestine.
618 *J. Pharm. Pharmacol.* **42**, 517–519 (1990).
619 47. Pappenheimer, J. R. & Reiss, K. Z. Contribution of solvent drag through intercellular
620 junctions to absorption of nutrients by the small intestine of the rat. *J. Membr. Biol.* **100**,
621 123–136 (1987).
622 48. Wishart, D. S. *et al.* HMDB: the Human Metabolome Database. *Nucleic Acids Res.* **35**,
623 D521–D526 (2007).
624 49. Wishart, D. S. *et al.* HMDB: a knowledgebase for the human metabolome. *Nucleic Acids*
625 *Res.* **37**, D603–D610 (2009).
626 50. Wishart, D. S. *et al.* HMDB 3.0—The Human Metabolome Database in 2013. *Nucleic*

627 *Acids Res.* **41**, D801–D807 (2012).
628 51. Wishart, D. S. *et al.* HMDB 4.0: the human metabolome database for 2018. *Nucleic*
629 *Acids Res.* **46**, D608–D617 (2018).
630 52. R Core Team. R: A Language and Environment for Statistical Computing. R Foundation
631 for Statistical Computing.
632 53. Gelius-Dietrich, G., Desouki, A. A., Fritzemeier, C. J. & Lercher, M. J. sybil – Efficient
633 constraint-based modelling in R. *BMC Syst. Biol.* **7**, 125 (2013).
634 54. IBM. IBM ILOG CPLEX Optimization Studio.
635 55. Gelius-Dietrich, G. cplexAPI: R Interface to C API of IBM ILOG CPLEX.
636 56. Wickham, H. *et al.* Welcome to the Tidyverse. *J. Open Source Softw.* **4**, 1686 (2019).
637 57. Wickham, H., François, R., Henry, L., Müller, K. & Vaughan, D. dplyr: A Grammar of
638 Data Manipulation.
639 58. Wickham, H. *Ggplot2: Elegant Graphics for Data Analysis*. (Springer-Verlag New York,
640 2016).
641 59. Linlin, Y. ggvenn: Draw Venn Diagram by 'ggplot2'.
642 60. Arnold, J. B. ggthemes: Extra Themes, Scales and Geoms for 'ggplot2'.
643 61. Wickham, H. & Seidel, D. scales: Scale Functions for Visualization.
644 62. Brunson, J. ggalluvial: Layered Grammar for Alluvial Plots. *J. Open Source Softw.* **5**,
645 2017 (2020).
646 63. Wickham, H., Hester, J., Chang, W. & Bryan, J. devtools: Tools to Make Developing R
647 Packages Easier.
648 64. Labarthe, S. *et al.* A mathematical model to investigate the key drivers of the
649 biogeography of the colon microbiota. *J. Theor. Biol.* **462**, 552–581 (2019).
650 65. Kettle, H., Louis, P. & Flint, H. J. Process-based modelling of microbial community
651 dynamics in the human colon. *J. R. Soc. Interface* **19**, 20220489 (2022).
652 66. Lin, C. *et al.* GutLogo: Agent-based modeling framework to investigate spatial and
653 temporal dynamics in the gut microbiome. *PLOS ONE* **13**, e0207072 (2018).
654 67. Clark, R. L. *et al.* Design of synthetic human gut microbiome assembly and butyrate

655 production. *Nat. Commun.* **12**, 3254 (2021).

656 68. Blachier, F., Beaumont, M. & Kim, E. Cysteine-derived hydrogen sulfide and gut health:
657 a matter of endogenous or bacterial origin. *Curr. Opin. Clin. Nutr. Metab. Care* **22**, 68–75
658 (2019).

659 69. Yong, S. J., Tong, T., Chew, J. & Lim, W. L. Antidepressive Mechanisms of Probiotics
660 and Their Therapeutic Potential. *Front. Neurosci.* **13**, 1361 (2020).

661 70. Otaru, N. *et al.* GABA Production by Human Intestinal Bacteroides spp.: Prevalence,
662 Regulation, and Role in Acid Stress Tolerance. *Front. Microbiol.* **12**, 656895 (2021).

663 71. Matsumoto, M. *et al.* Colonic Absorption of Low-Molecular-Weight Metabolites
664 Influenced by the Intestinal Microbiome: A Pilot Study. *PLOS ONE* **12**, e0169207 (2017).

665 72. Canyelles, M. *et al.* Gut Microbiota-Derived TMAO: A Causal Factor Promoting
666 Atherosclerotic Cardiovascular Disease? *Int. J. Mol. Sci.* **24**, 1940 (2023).

667 73. Oliphant, K. & Allen-Vercoe, E. Macronutrient metabolism by the human gut microbiome:
668 major fermentation by-products and their impact on host health. *Microbiome* **7**, 91
669 (2019).

670 74. Ma, N. & Ma, X. Dietary Amino Acids and the Gut-Microbiome-Immune Axis:
671 Physiological Metabolism and Therapeutic Prospects. *Compr. Rev. Food Sci. Food Saf.*
672 **18**, 221–242 (2019).

673 75. Chen, Y. *et al.* Absorptive transport of amino acids by the rat colon. *Am. J. Physiol.-*
674 *Gastrointest. Liver Physiol.* **318**, G189–G202 (2020).

675 76. Li, T.-T. *et al.* Microbiota metabolism of intestinal amino acids impacts host nutrient
676 homeostasis and physiology. *Cell Host Microbe* **32**, 661-675.e10 (2024).

677 77. Kostopoulos, I. *et al.* A Continuous Battle for Host-Derived Glycans Between a Mucus
678 Specialist and a Glycan Generalist in vitro and in vivo. *Front. Microbiol.* **12**, 632454
679 (2021).

680

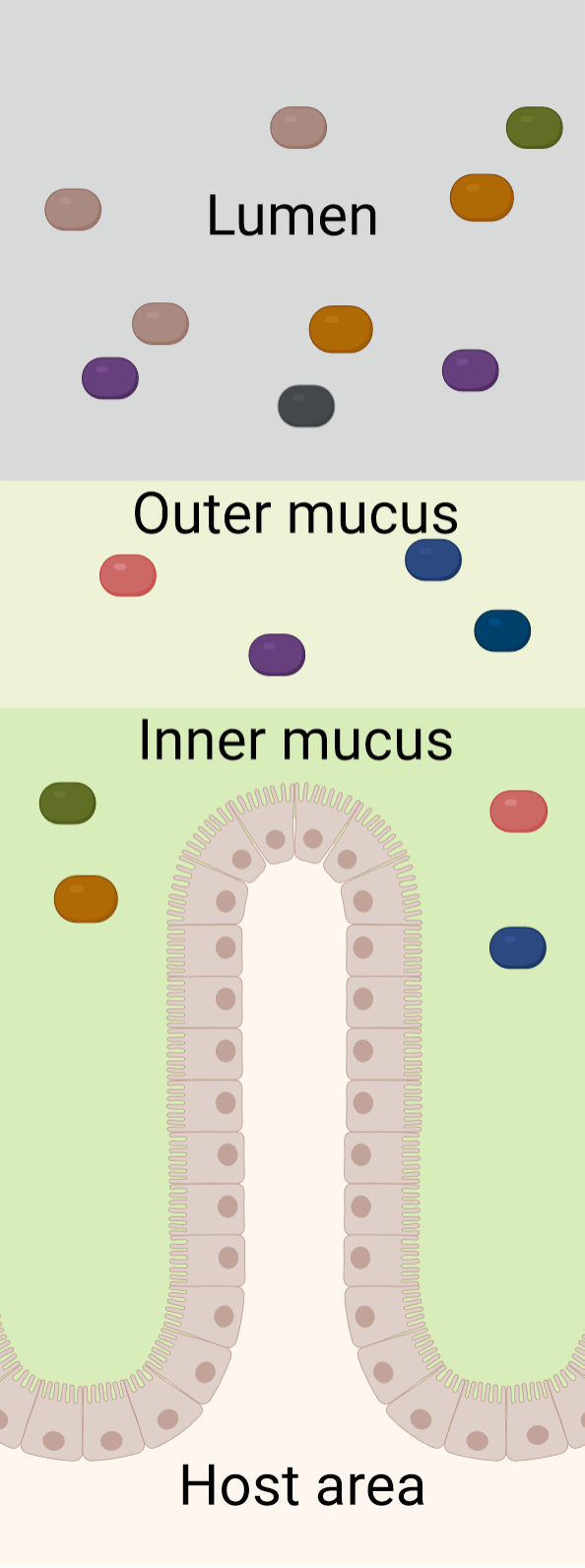
Lumen
Outer mucus
Inner mucus
Host area

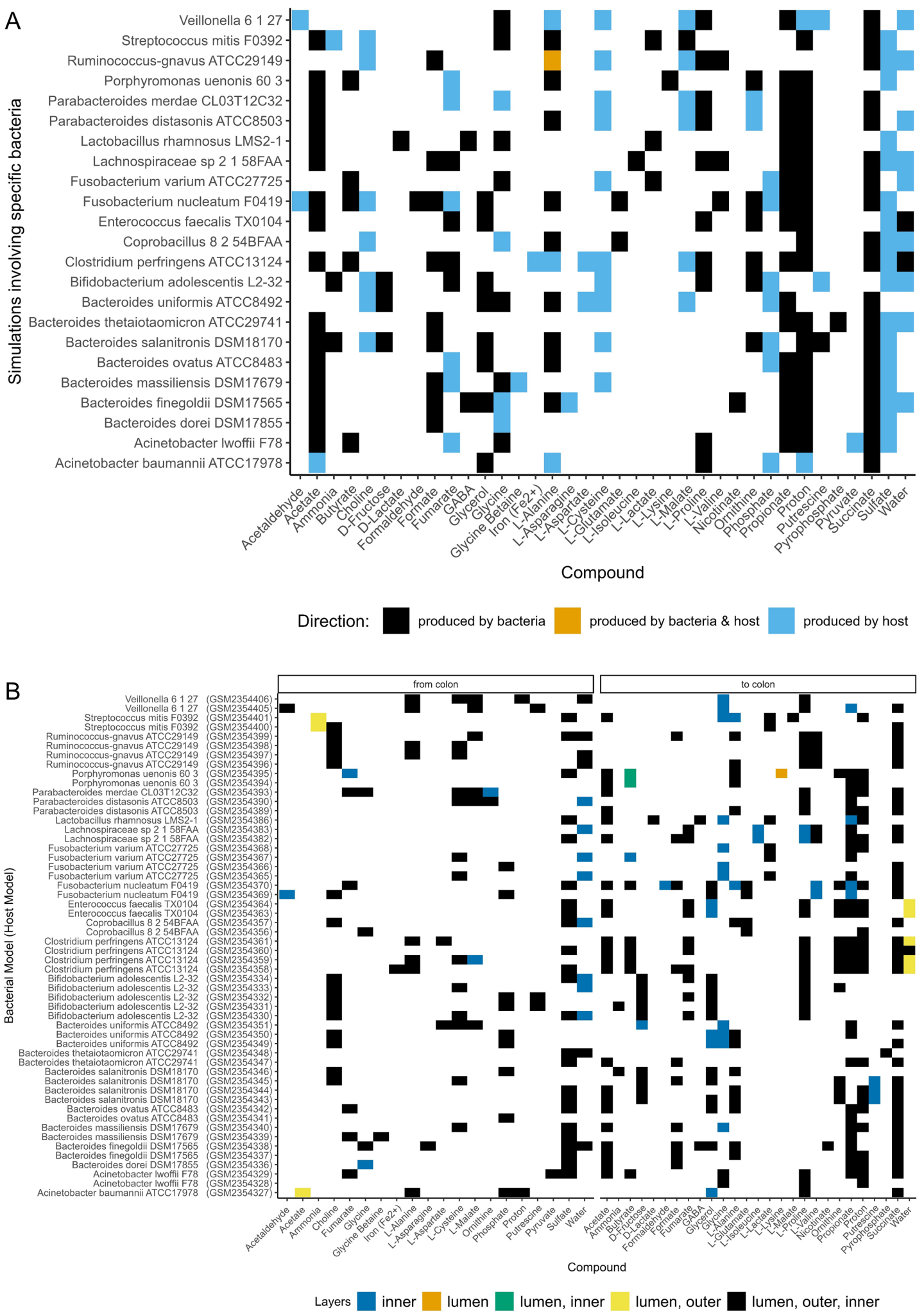
A
Simulations involving specific bacteria
Veillonella 6 1 27
Streptococcus mitis F0392
Ruminococcus-gnavus ATCC29149
Porphyromonas uenonis 60 3
Parabacteroides merdae CL03T12C32
Parabacteroides distasonis ATCC8503
Lactobacillus rhamnosus LMS2-1
Lachnospiraceae sp 2 1 58FAA
Fusobacterium varium ATCC27725
Fusobacterium nucleatum F0419
Enterococcus faecalis TX0104
Coprobacillus 8 2 54BFAA
Clostridium perfringens ATCC13124
Bifidobacterium adolescentis L2-32
Bacteroides uniformis ATCC8492
Bacteroides thetaiotaomicron ATCC29741
Bacteroides salanitronis DSM18170
Bacteroides ovatus ATCC8483
Bacteroides massiliensis DSM17679
Bacteroides finegoldii DSM17565
Bacteroides dorei DSM17855
Acinetobacter lwoffii F78
Acinetobacter baumannii ATCC17978
Acetaldehyde
Acetate
Ammonia
Butyrate
Choline
D-Fructose
D-Lactate
Formaldehyde
Formate
Fumarate
GABA
Glycerol
Glycine
Glycine Betaine
Iron (Fe2+)
L-Alanine
L-Asparagine
L-Aspartate
L-Cysteine
L-Glutamate
L-Isoleucine
L-Lactate
L-Lysine
L-Malate
L-Proline
L-Valine
Nicotinate
Ornithine
Phosphate
Propionate
Proton
Putrescine
Pyrophosphate
Pyruvate
Succinate
Sulfate
Water
Compound
Direction:
produced by bacteria
produced by bacteria & host
produced by host
B
Bacterial Model (Host Model)
from colon
to colon
Veillonella 6 1 27 (GSM2354406)
Veillonella 6 1 27 (GSM2354405)
Streptococcus mitis F0392 (GSM2354401)
Streptococcus mitis F0392 (GSM2354400)
Ruminococcus-gnavus ATCC29149 (GSM2354399)
Ruminococcus-gnavus ATCC29149 (GSM2354398)
Ruminococcus-gnavus ATCC29149 (GSM2354397)
Ruminococcus-gnavus ATCC29149 (GSM2354396)
Porphyromonas uenonis 60 3 (GSM2354395)
Porphyromonas uenonis 60 3 (GSM2354394)
Parabacteroides merdae CL03T12C32 (GSM2354393)
Parabacteroides distasonis ATCC8503 (GSM2354390)
Parabacteroides distasonis ATCC8503 (GSM2354389)
Lactobacillus rhamnosus LMS2-1 (GSM2354386)
Lachnospiraceae sp 2 1 58FAA (GSM2354383)
Lachnospiraceae sp 2 1 58FAA (GSM2354382)
Fusobacterium varium ATCC27725 (GSM2354368)
Fusobacterium varium ATCC27725 (GSM2354367)
Fusobacterium varium ATCC27725 (GSM2354366)
Fusobacterium varium ATCC27725 (GSM2354365)
Fusobacterium nucleatum F0419 (GSM2354370)
Fusobacterium nucleatum F0419 (GSM2354369)
Enterococcus faecalis TX0104 (GSM2354364)
Enterococcus faecalis TX0104 (GSM2354363)
Coprobacillus 8 2 54BFAA (GSM2354357)
Coprobacillus 8 2 54BFAA (GSM2354356)
Clostridium perfringens ATCC13124 (GSM2354361)
Clostridium perfringens ATCC13124 (GSM2354360)
Clostridium perfringens ATCC13124 (GSM2354359)
Clostridium perfringens ATCC13124 (GSM2354358)
Bifidobacterium adolescentis L2-32 (GSM2354334)
Bifidobacterium adolescentis L2-32 (GSM2354333)
Bifidobacterium adolescentis L2-32 (GSM2354332)
Bifidobacterium adolescentis L2-32 (GSM2354331)
Bifidobacterium adolescentis L2-32 (GSM2354330)
Bacteroides uniformis ATCC8492 (GSM2354351)
Bacteroides uniformis ATCC8492 (GSM2354350)
Bacteroides uniformis ATCC8492 (GSM2354349)
Bacteroides thetaiotaomicron ATCC29741 (GSM2354348)
Bacteroides thetaiotaomicron ATCC29741 (GSM2354347)
Bacteroides salanitronis DSM18170 (GSM2354346)
Bacteroides salanitronis DSM18170 (GSM2354345)
Bacteroides salanitronis DSM18170 (GSM2354344)
Bacteroides salanitronis DSM18170 (GSM2354343)
Bacteroides ovatus ATCC8483 (GSM2354342)
Bacteroides ovatus ATCC8483 (GSM2354341)
Bacteroides massiliensis DSM17679 (GSM2354340)
Bacteroides massiliensis DSM17679 (GSM2354339)
Bacteroides finegoldii DSM17565 (GSM2354338)
Bacteroides finegoldii DSM17565 (GSM2354337)
Bacteroides dorei DSM17855 (GSM2354336)
Acinetobacter lwoffii F78 (GSM2354329)
Acinetobacter lwoffii F78 (GSM2354328)
Acinetobacter baumannii ATCC17978 (GSM2354327)
Acetaldehyde
Acetate
Ammonia
Choline
Fumarate
Glycine
Glycine Betaine
Iron (Fe2+)
L-Alanine
L-Asparagine
L-Aspartate
L-Cysteine
L-Malate
Ornithine
Phosphate
Proton
Putrescine
Pyruvate
Sulfate
Water
Acetate
Ammonia
Butyrate
D-Fructose
D-Lactate
Formaldehyde
Formate
Fumarate
GABA
Glycerol
Glycine
L-Alanine
L-Glutamate
L-Isoleucine
L-Lactate
L-Lysine
L-Malate
L-Proline
L-Valine
Nicotinate
Ornithine
Propionate
Proton
Putrescine
Pyrophosphate
Succinate
Water
Compound
Layers
inner
lumen
lumen, inner
lumen, outer
lumen, outer, inner

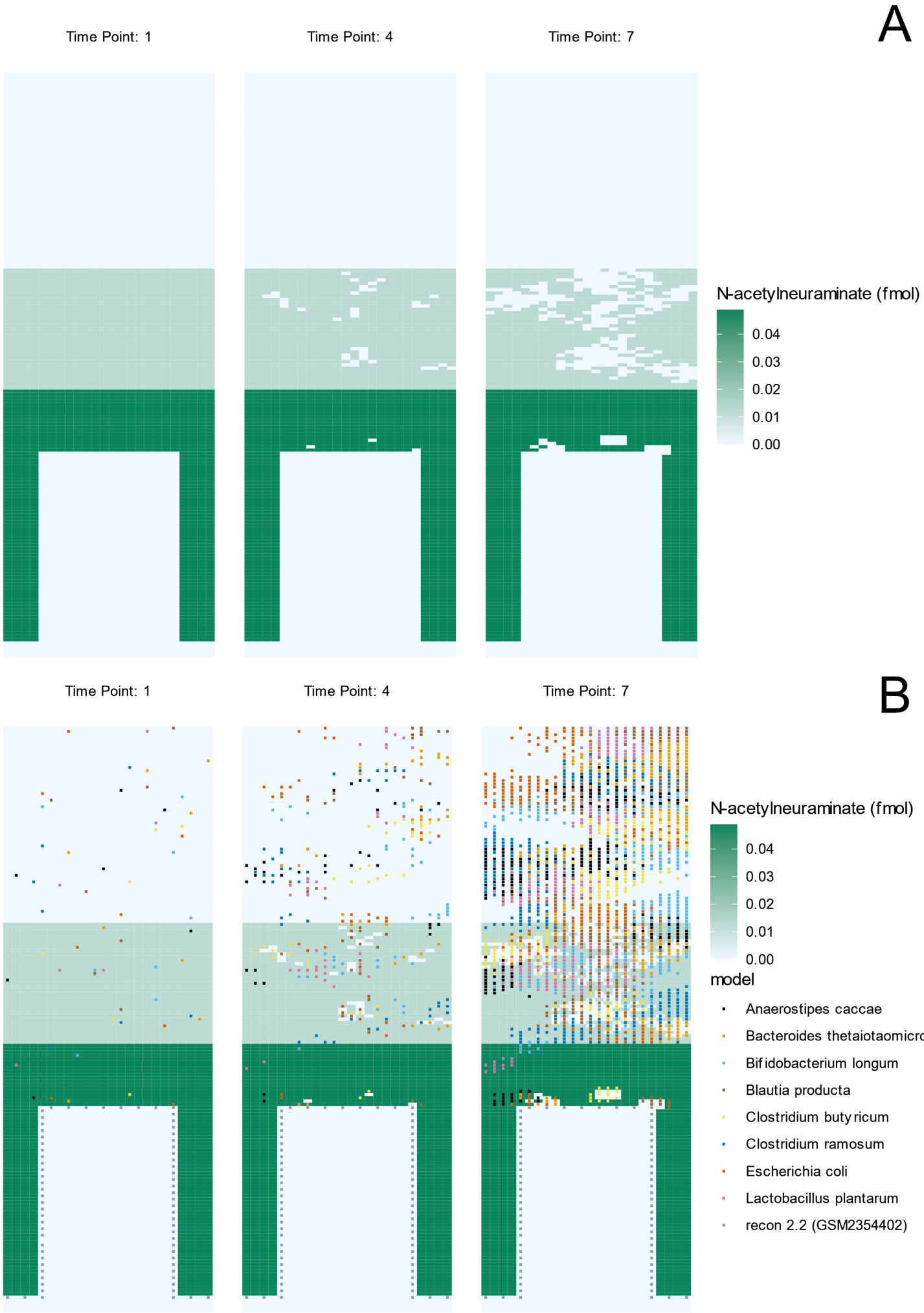
A
Time Point: 1
Time Point: 4
Time Point: 7
N-acetylneuraminate (fmol)
0.04
0.03
0.02
0.01
0.00
B
Time Point: 1
Time Point: 4
Time Point: 7
N-acetylneuraminate (fmol)
0.04
0.03
0.02
0.01
0.00
model
Anaerostipes caccae
Bacteroides thetaiotaomicro
Bifidobacterium longum
Blautia producta
Clostridium butyricum
Clostridium ramosum
Escherichia coli
Lactobacillus plantarum
recon 2.2 (GSM2354402)

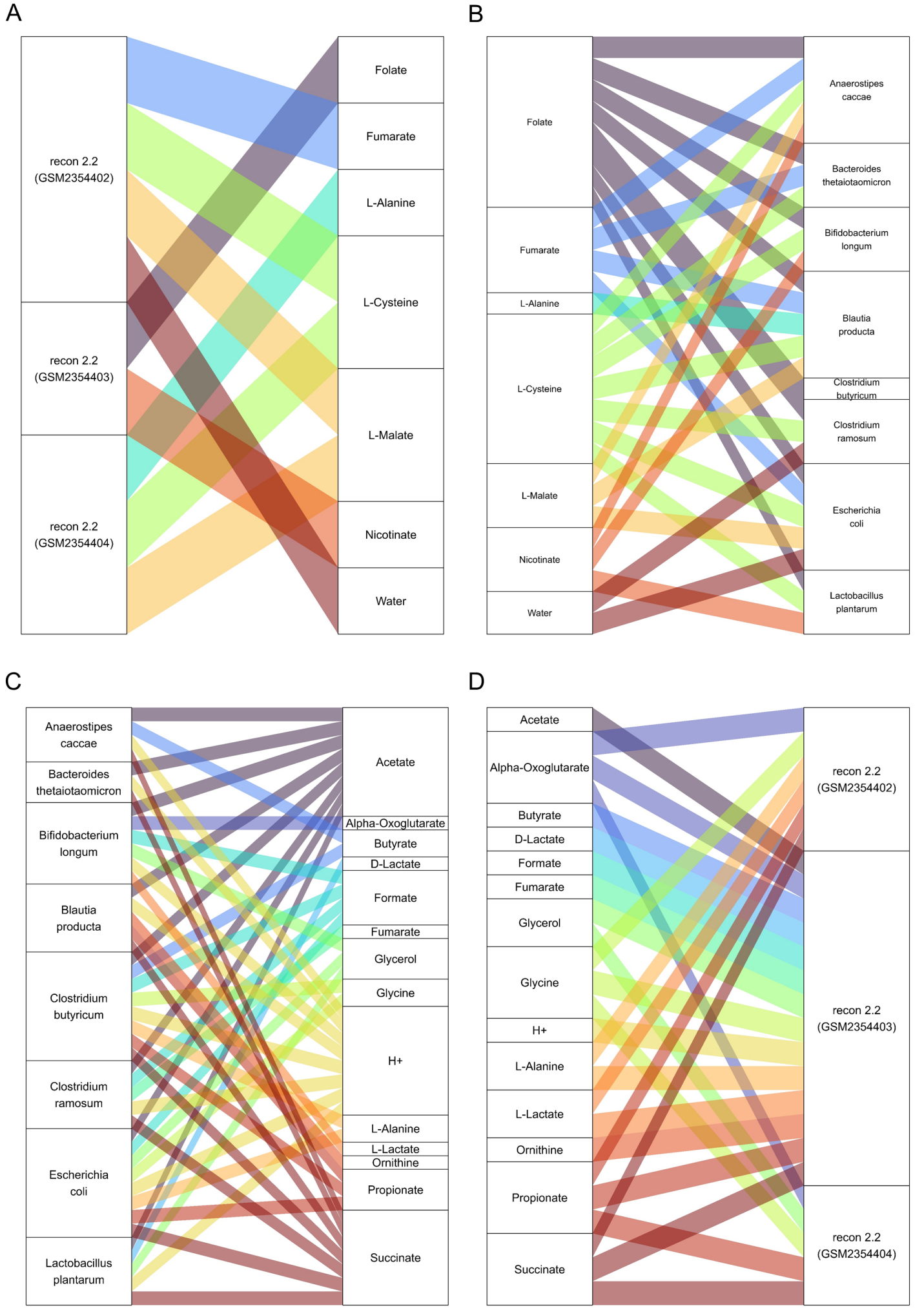
A
recon 2.2 (GSM2354402)
recon 2.2 (GSM2354403)
recon 2.2 (GSM2354404)
Folate
Fumarate
L-Alanine
L-Cysteine
L-Malate
Nicotinate
Water
B
Folate
Fumarate
L-Alanine
L-Cysteine
L-Malate
Nicotinate
Water
Anaerostipes caccae
Bacteroides thetaiotaomicron
Bifidobacterium longum
Blautia producta
Clostridium butyricum
Clostridium ramosum
Escherichia coli
Lactobacillus plantarum
C
Anaerostipes caccae
Bacteroides thetaiotaomicron
Bifidobacterium longum
Blautia producta
Clostridium butyricum
Clostridium ramosum
Escherichia coli
Lactobacillus plantarum
Acetate
Alpha-Oxoglutarate
Butyrate
D-Lactate
Formate
Fumarate
Glycerol
Glycine
H+
L-Alanine
L-Lactate
Ornithine
Propionate
Succinate
D
Acetate
Alpha-Oxoglutarate
Butyrate
D-Lactate
Formate
Fumarate
Glycerol
Glycine
H+
L-Alanine
L-Lactate
Ornithine
Propionate
Succinate
recon 2.2 (GSM2354402)
recon 2.2 (GSM2354403)
recon 2.2 (GSM2354404)

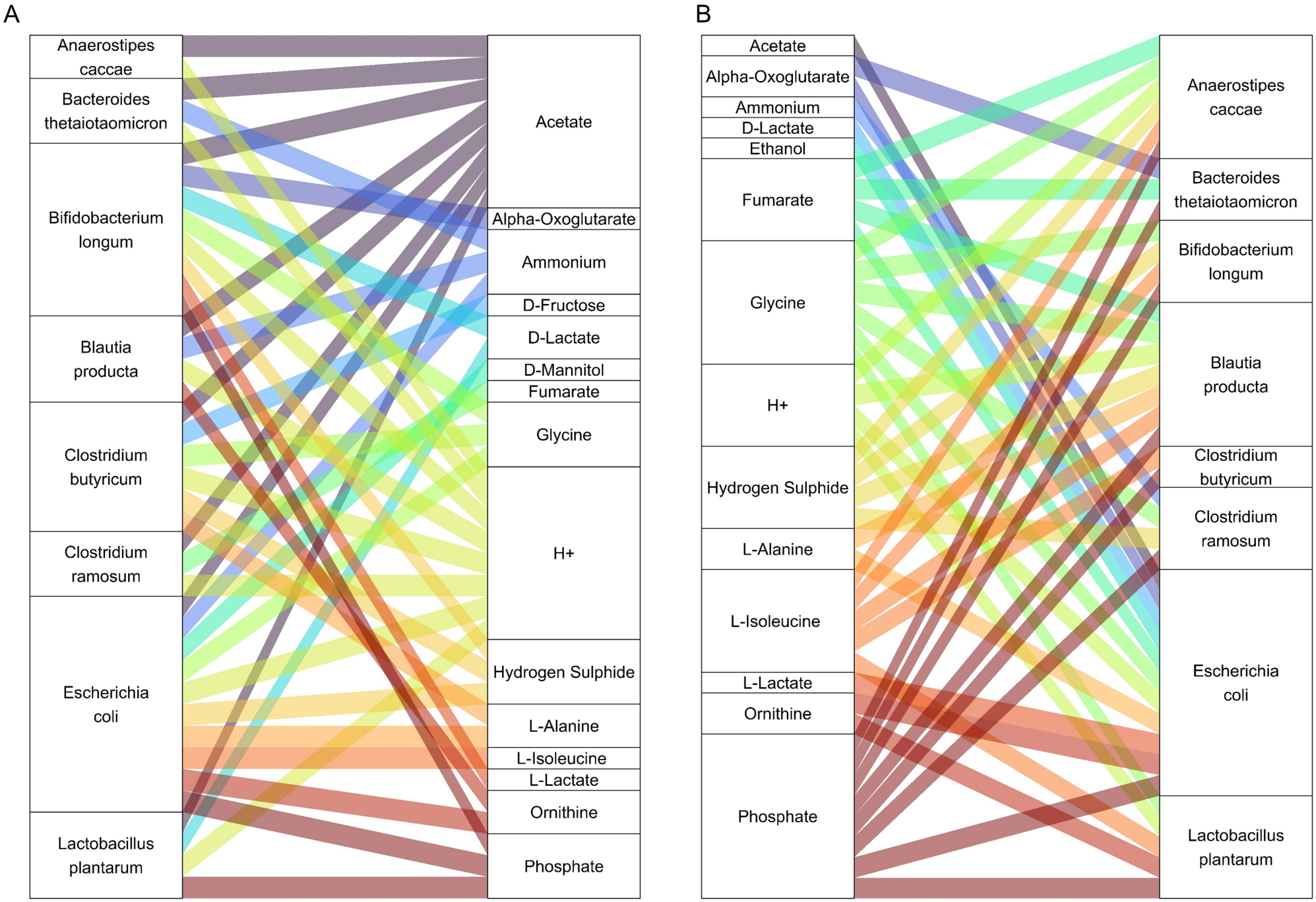
A
Anaerostipes caccae
Bacteroides thetaiotaomicron
Bifidobacterium longum
Blautia producta
Clostridium butyricum
Clostridium ramosum
Escherichia coli
Lactobacillus plantarum
Acetate
Alpha-Oxoglutarate
Ammonium
D-Fructose
D-Lactate
D-Mannitol
Fumarate
Glycine
H+
Hydrogen Sulphide
L-Alanine
L-Isoleucine
L-Lactate
Ornithine
Phosphate
B
Acetate
Alpha-Oxoglutarate
Ammonium
D-Lactate
Ethanol
Fumarate
Glycine
H+
Hydrogen Sulphide
L-Alanine
L-Isoleucine
L-Lactate
Ornithine
Phosphate
Anaerostipes caccae
Bacteroides thetaiotaomicron
Bifidobacterium longum
Blautia producta
Clostridium butyricum
Clostridium ramosum
Escherichia coli
Lactobacillus plantarum

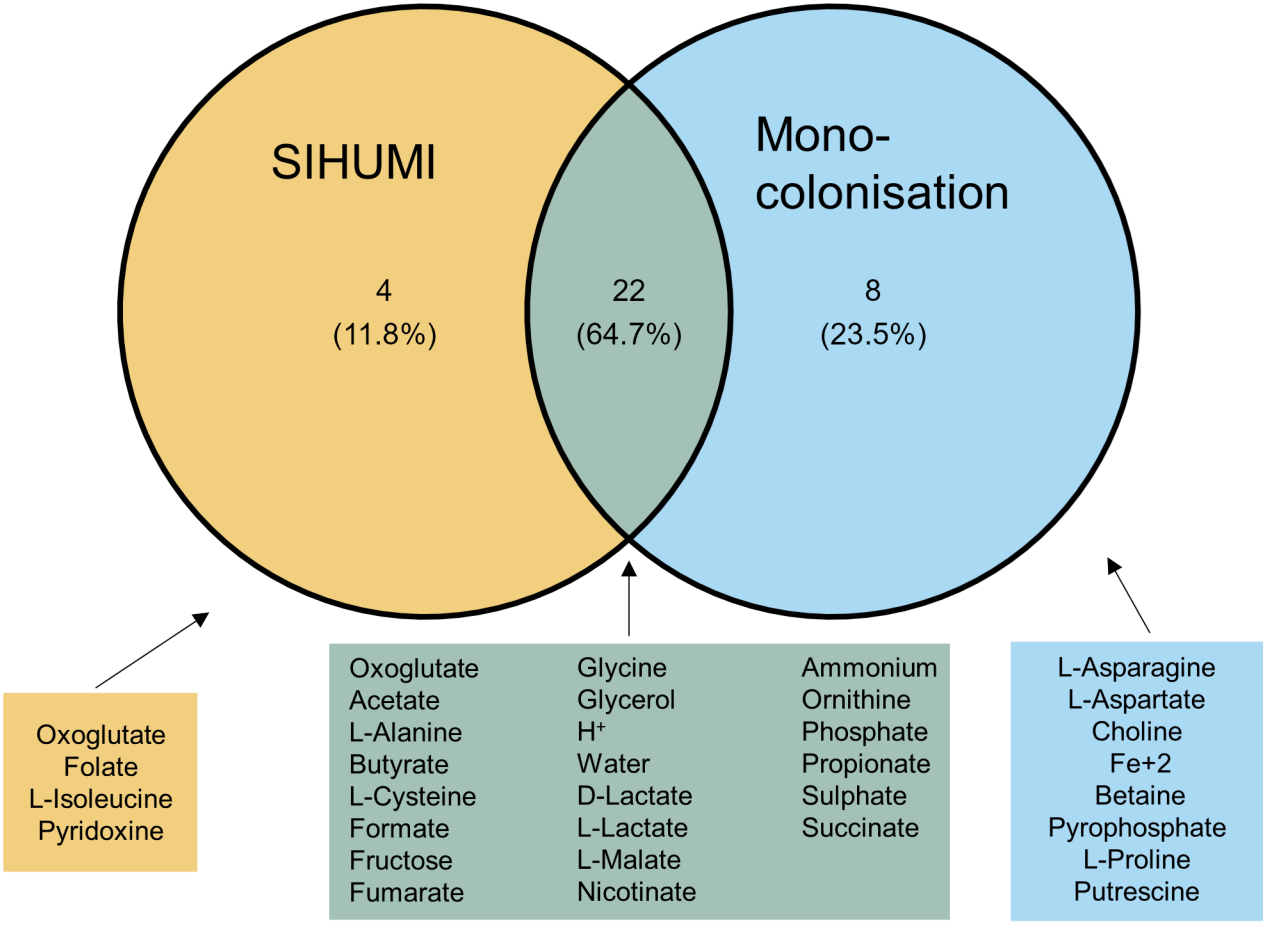
SIHUMI
Mono-colonisation
4
(11.8%)
22
(64.7%)
8
(23.5%)
Oxoglutate
Folate
L-Isoleucine
Pyridoxine
Oxoglutate
Acetate
L-Alanine
Butyrate
L-Cysteine
Formate
Fructose
Fumarate
Glycine
Glycerol
H+
Water
D-Lactate
L-Lactate
L-Malate
Nicotinate
Ammonium
Ornithine
Phosphate
Propionate
Sulphate
Succinate
L-Asparagine
L-Aspartate
Choline
Fe+2
Betaine
Pyrophosphate
L-Proline
Putrescine